USGS Award Number 05HQGR0160

Principal Investigator: G. Lang Farmer, University of Colorado, Boulder
Other project personnel; Rich Goldfarb (USGS), Craig Hart (Univ. Western Australia), Erin Marsh (USGS), John Mair (Univ. British Columbia)

Final Technical Report for " Petrogenesis of Cretaceous, Gold-Related Plutons, Eastern Tintina Gold Province (TGP), Alaska and Yukon: Implications for Ore Genesis and Resource Distribution in the Northern Cordillera"

"Research supported by the U.S. Geological Survey (USGS), Department of the Interior, under USGS award number 05HQGR0160. *The views and conclusions contained in this document are those of the authors and should not be interpreted as necessarily representing the official policies, either expressed or implied, of the U.S. Government."*

Technical Report

Research activities for this award were centered around two projects; the petrogenesis of gold related Late Cretaceous intrusive igneous rocks at Scheelite Dome, at the eastern end of the Eastern Tintina Gold Province, and detailed microsample studies of intrusive rocks of the Late Cretaceous Fort Knox pluton in central Alaska. These studies are described separately in the following text.

Petrogenesis of Late Cretaceous Scheelite Dome Intrusive Complex, Yukon

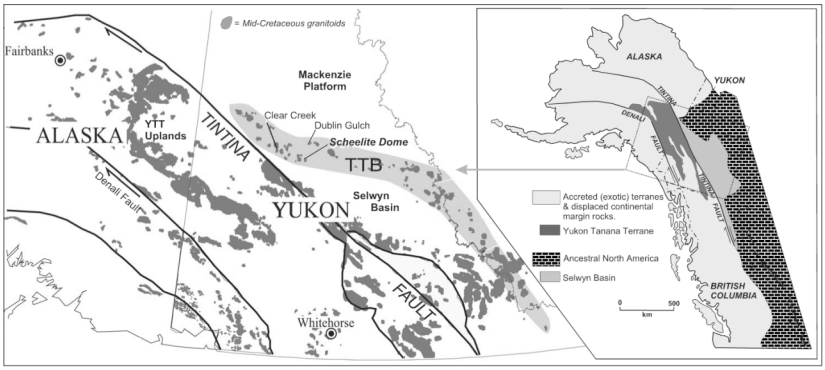

Fig. 1 Regional geological setting of the northern Cordillera of Alaska (USA) and Yukon (Canada), highlighting the extent and distribution of mid-Cretaceous plutonic belts. The major phase of collision, accretion, and outgrowth of the continental margin took place from the Early Jurassic to mid-Cretaceous. Dextral strike-slip movement on the Tintina and Denali fault systems commenced in the Late Cretaceous after the cessation of mid-Cretaceous magmatism. At approximately 115 to 90 Ma, the YTT Uplands of east-central Alaska was positioned immediately south of the western Tombstone Tungsten magmatic belt (TTB), which is the youngest, and most inboard, or cratonward, of the mid-Cretaceous plutonic belts.

The following text is excerpted and modified from a completed manuscript to be submitted to the Journal of Petrology entitled "Scheelite Dome intrusive complex, Tombstone-Tungsten magmatic belt, Yukon", by Mair, Farmer, et al. The paper represents some of the work undertaken as part of this award, and presents some of the first petrologic and geochemical of the intrusive igneous rocks associated with gold deposition at Scheelite Dome.

The Scheelite Dome area, central Yukon, Canada (Fig. 1), is underlain by deformed and weakly metamorphosed rocks of the ancestral North American continental margin, which has been intruded by compositionally diverse stocks and dykes at 93 ± 3 Ma. Plutonism took place in a post collisional regime that followed the collision and accretion of outboard terranes with the continental margin. Similar to other spatially and

temporally related intrusive centers, the Scheelite Dome intrusions are associated with reduced intrusion-related gold deposits.

Intrusions range from volumetrically dominant clinopyroxene-bearing monzogranites and calc-alkaline minettes and spessartites, but also include leucominettes, quartz monzonites, quartz monzodiorites and granodiorites (Fig. 2). Irregular and commonly intermingled contacts between successive intrusive phases and existing geochronologic data (Mair et al, in press) indicate that all phases were emplaced during a single short-lived magmatic episode. All rock types are potassic (Fig. 3), are strongly enriched in LILEs and LREEs, and feature high LILE/HFSE ratios (Fig. 4). Clinopyroxene is common to all rock types, and ranges from salite in felsic rocks to high-Mg augite and Cr-rich diopside in lamprophyres. Less common, calcic amphibole ranges from actinolitic hornblende to pargasite. The rocks have strongly radiogenic Sr (initial $^{87}Sr/^{86}Sr$

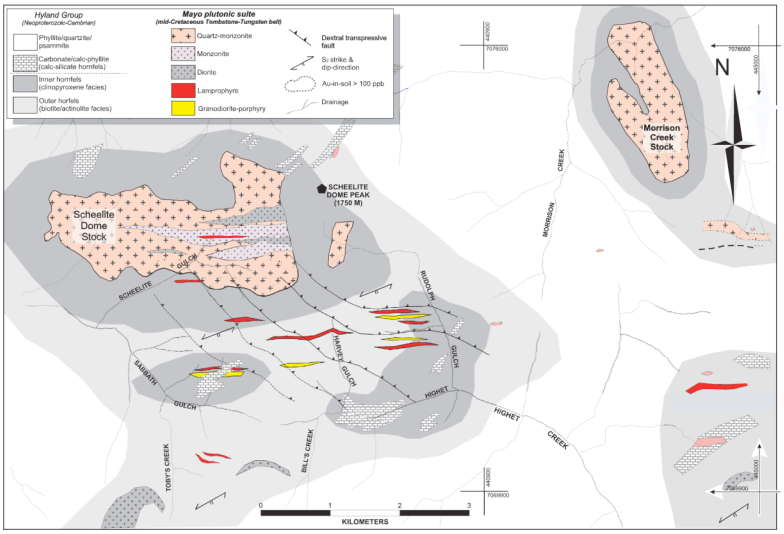

Fig. 2 Generalized geology of the Scheelite Dome area. Two main quartz monzonite stocks and numerous felsic to mafic dykes intrude strongly deformed rocks of the Neoproterozoic Hyland Group. Dykes are mostly hosted in E-trending tensional zones. The distribution of intrusions and hornfels suggests that the exposure level is near the apices of the intrusive complex. A variety of gold- and tungsten-rich reduced skarns and veins occur within the extensive Au-in-soil anomaly. Co-ordinates are in UTM (zone 8).

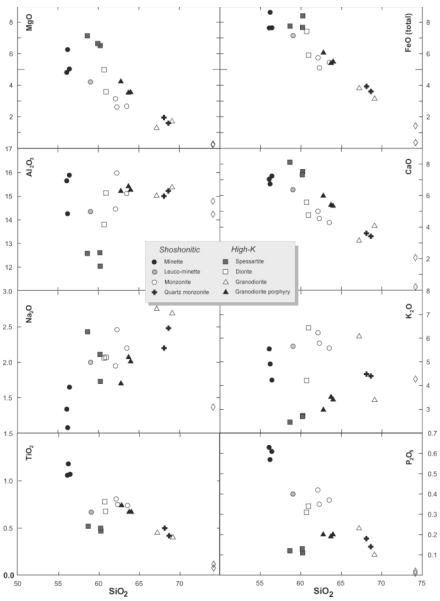

Fig. 3 Major element Harker variation diagrams for intrusive rocks at Scheelite Dome. Major element compositions are normalized to 100% volatile free.

0.711-0.714) and Pb isotope ratios ($^{206}Pb/^{204}Pb$ 19.2 – 19.7), and negative initial ε_{Nd} values (-8.06 to –11.26), as compiled in Table 1 and depicted in Fig. 5. The Nd and Sr isotopic compositions are essentially equivalent to those of Late Cretaceous, gold-mineralization related, intrusive igneous rocks further to the west in the Fairbanks areas (Table 2).

Collectively, the data suggest close genetic relationships between all rock types. Whole rock major and trace element, radiogenic isotope and textural and mineralogical data suggest that monzogranites and quartz monzonites evolved from mafic potassic magmas sourced from the lithospheric mantle via assimilation of metasedimentary

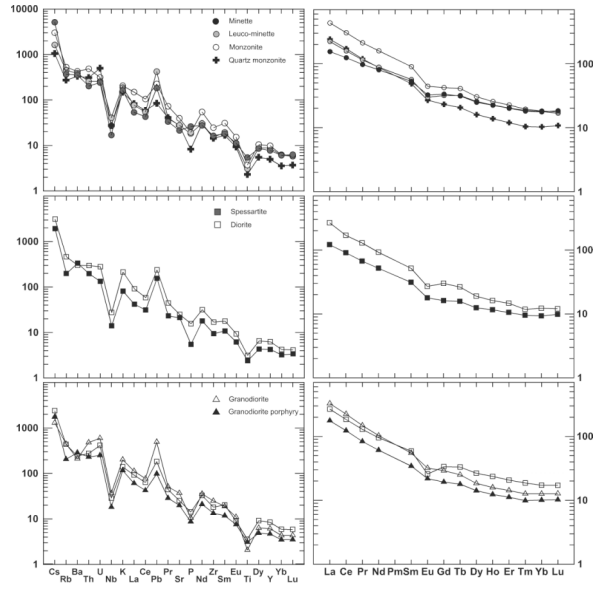

Fig. 4- A) Trace element spider diagrams normalized to the primitive mantle values of Sun and McDonough (1989). A representative sample of each rock type is plotted. Trace element characteristics across the compositional range of intrusions are remarkably uniform. All samples are strongly enriched in incompatible elements, particularly LILEs and light REEs, and feature high LIL/HSFE ratios. B) Rare earth element spider diagrams normalized to the chondritic values of Sun and McDonough (1989). A representative sample of each rock type is plotted.

SAMPLE	Rb ppm	Sr ppm	$^{87}Rb/^{86}Sr$	$^{87}Sr/^{86}Sr_m$		$^{87}Sr/^{86}Sr_{(T)}$	Sm ppm	Nd ppm	$^{143}Nd/^{144}Nd_m$		$^{143}Nd/^{144}Nd_{(T)}$	$\varepsilon_{Nd}(T)$	T_{DM}	$^{208}Pb/^{204}Pb$	$^{207}Pb/^{204}Pb$	$^{206}Pb/^{204}Pb$	$\delta^{18}O$
Quartz monzonite																	
SD-Main	169.5	602.2	0.8134	0.713574	7	0.71251	7.43	41.8	0.512068	13	0.512003	-10.07	1.40	39.168	15.675	19.432	*12.1*
Monzonite																	
SD-104 PC	300.4	812.0	1.0693	0.714026	39	0.71263	13.08	73.0	0.512008	15	0.511943	-11.26	1.50	39.419	15.728	19.456	11.7
SD-104-PC K-spar	209.1	1250.0	0.4834	0.713667	17	0.71304	0.14	0.6	0.512018	8	0.511935	-11.40	2.04	38.954	15.665	19.107	12.6
SD-104-PC Cpx	3.4	44.9	0.2190	0.712758	12	0.71247	32.53	175.4	0.512012	17	0.511944	-11.22	1.54	-	-	-	10.4
Leuco-minette																	
SD-103 B	248.5	552.5	1.2999	0.713472	9	0.71177	8.09	38.9	0.512122	12	0.512046	-9.23	1.59	39.036	15.669	19.258	11.4
Quartz monzodiorite																	
SD-102-1	233.9	509.3	1.3273	0.713588	13	0.71185	8.62	43.9	0.512083	13	0.512011	-9.91	1.54	39.215	15.694	19.627	11.5
SD-102-2	322.9	617.0	1.5126	0.714606	12	0.71263	9.22	51.5	0.512035	11	0.511970	-10.73	1.46	39.385	15.695	19.530	9.7
Bill's Creek	164.7	419.9	1.1333	0.715496	11	0.71401	6.49	35.8	0.512144	15	0.512078	-8.62	1.32	39.813	15.724	20.040	12.9
Granodiorite																	
TZ-Dike	229.1	745.1	0.8887	0.713040	9	0.71188	7.97	46.8	0.512048	8	0.511986	-10.41	1.37	39.139	15.671	19.381	12.5
Lamprophyre - Minette																	
Minette	206.8	441.4	1.3541	0.713515	11	0.71174	7.82	37.1	0.512067	15	0.511990	-10.33	1.72	39.370	15.722	19.420	5.2 - 5.6
East Ridge Minette (ERM)	210.6	480.0	1.2681	0.715883	9	0.71423	7.66	37.1	0.512086	7	0.512011	-9.93	1.64	39.362	15.708	19.444	10.6
ERM - Cpx	36.6	137.3	0.7693	0.714407	9	0.71340	10.69	51.0	0.51209	7	0.512014	-9.87	1.67	-	-	-	9.6
ERM - Apatite	223.7	1377.0	0.4694	0.713576	12	0.71296	0.71	4.2	0.512068	8	0.512006	-10.02	1.34	39.229	15.693	19.439	
ERM - K-spar	310.4	415.5	2.1591	0.716798	13	0.71398	0.68	3.5	0.512068	8	0.511998	-10.18	1.52	39.156	15.681	19.297	12.3
Lamprophyre - Spessartite																	
SD-104A	107.9	812.0	0.3841	0.714026	39	0.71352	4.46	23.3	0.512176	27	0.512106	-8.06	1.35	39.063	15.691	19.324	11.7
SD-103 A	151.5	419.8	1.0427	0.712908	14	0.71154	4.68	25.1	0.512164	17	0.512096	-8.27	1.33	39.250	15.704	19.525	10.8

Table 1- Table showing isotope dilution Rb, Sr, Sm, and Nd concentrations and Nd, Sr, Pb and O isotopic compositions of Scheelite Dome igneous rocks.

crust and fractional crystallization. Leucominette and quartz monzodiorite to

Location	SAMPLE	Ref.	Age	Rb	Sr	$^{87}Rb/^{86}Sr$	$^{87}Sr/^{86}Sr_{m}$	$^{87}Sr/^{86}Sr_{(T)}$	Sm	Nd	$^{143}Nd/^{144}Nd_{m}$	$^{143}Nd/^{144}Nd_{(T)}$	$\varepsilon_{Nd}(T)$	T_{DM}	$^{208}Pb/^{204}Pb$	$^{207}Pb/^{204}Pb$	$^{206}Pb/^{204}Pb$	$\delta^{18}O$
Selwyn Basin*	QMS	1	580?	132	129	2.971	0.7333	0.72910	-	-	-	-	-	-	-	-	-	-
(Hyland Group)	QMS	1	580?	321	134	6.985	0.7620	0.75216	-	-	-	-	-	-	-	-	-	-
	QMS	1	580?	17	90	0.563	0.7514	0.75060	-	-	-	-	-	-	-	-	-	-
	QMS	1	580?	205	135	4.414	0.7510	0.74476	-	-	-	-	-	-	-	-	-	-
	QMS	1	580?	144	72	5.844	0.7628	0.75455	-	-	-	-	-	-	-	-	-	-
Selwyn Basin 2*	S	2	580	-	-	-	-	-	5.16	33.1	0.511229	0.511229	-26.2	2.3	-	-	-	-
(Hyland Group)	S	2	580	-	-	-	-	-	3.33	16.7	0.511316	0.511316	-24.8	2.9	-	-	-	-
	S	2	575	-	-	-	-	-	6.58	37.2	0.511381	0.511381	-23.4	2.4	-	-	-	-
	S	2	575	-	-	-	-	-	1.15	6.3	0.511416	0.511416	-22.7	2.4	-	-	-	-
	S	2	570	-	-	-	-	-	4.47	26.6	0.511483	0.511483	-21.3	2.1	-	-	-	-
	S	3		-	-	-	-	-	-	-	-	-	-	-	-	-	-	14 - 16
Fairbanks	Gtd	4	92	119	909	0.373	0.7123	0.71184	-	-	-	-	-	-	18.99	15.61	18.99	-
	Gtd	4	92	109	601	0.517	0.7128	0.71208	-	-	-	-	-	-	-	-	-	-
	Gtd	4	92	248	338	2.091	0.7124	0.70963	-	-	-	-	-	-	-	-	-	-
	Gtd	5	92	82	407	-	-	0.71190	-	-	-	-	-10.7	1.5	-	-	-	-
	(range)			126	1190	-	-	0.71460	-	-	-	-	-11.6	1.7	-	-	-	-
YTT Uplands			93	98	277	-	0.7119	0.71052	3.40	17.9	0.512084	0.512014	-9.8	1.5	-	-	-	-
	Gtd	6	94	102	335	-	0.7110	0.70978	3.26	17.8	0.512069	0.512001	-10.1	1.4	19.25	15.68	39.15	-
	Gtd	6	101	181	360	-	0.7218	0.71970	4.68	25.3	0.511701	0.511627	-15.1	1.8	19.27	15.67	39.14	8.4
	Gtd	6	110	148	257	-			5.28	29.9	0.511803	0.511726	-16.3	1.8	19.41	15.72	39.44	-
	Gtd	6	115	216	157	-	0.7478	0.74131	4.09	18.0	0.511497	0.511394	-21.4	3.1	19.39	15.72	39.40	11.1
Cassiar Batholith	BtMsGr	7	100	119	70	1.000	0.7118	0.70928	2.45	10.7	0.511734	0.511591	-17.1	1.3	39.14	15.70	19.14	7.6
	(range)			252	390	8.400	0.7455	0.73360	7.11	39.7	0.512253	0.512140	-6.3	N.D.	39.26	15.71	19.22	11.6
	BtGr	7	100	103	437	0.570	0.7071	0.70616	3.33	19.2	0.512323	0.512223	-3.0	1.1	39.22	15.72	19.22	9.4
	(range)			127	601	0.782	0.7083	0.70717	10.10	46.9	0.512414	0.512313	-4.8	1.4	-	-	-	10.2
	BtHbGtd	7	100	84	363	0.249	0.7063	0.70598	4.21	23.1	0.512274	0.512162	-6.0	1.0	-	-	-	-
	(range)			128	1102	2.076	0.7122	0.70923	9.69	62.1	0.512432	0.512330	-2.7	1.4	-	-	-	-

Ref = References: 1 = Kuran et al., (1983); 2 = Garzione et al., (1997); 3 = Mair et al. (in review); 4 = Newberry and Solie (1997); 5 = Haynes et al. (2005); 6 = Allenikoff et al., (2000);7 = Driver et al., (2000)
QMS = quartz-muscovite schist; S = schist (undifferentiated); Gtd= Granitoid (undifferentiated); BtMsGr = biotite-muscovite granite
BtGtd = biotite granitoid; BtHbGtd = biotite-hornblende granodiorite
* = Initial isotope ratios for (meta) sedimentary rocks are calculated at 100 Ma., to aid in comparisons to ca. 115-90 Ma. granitoids.

Table 2- Regional compilation of Nd, Sr and Pb isotopic data from Late Cretaceous intrusive rocks and bedrock from Yukon and central Alaska.

granodiorite dykes reflect hybrid rocks developed by the interaction of new influxes of mantle-derived magma with more evolved magma, and subsequent differentiation. Largely unmodified minettes and spessartites represent the most primitive and final phases emplaced. A crust dominated by metasedimentary strata, in conjunction with long-lived metasomatic enrichments in the underlying lithospheric mantle are attributes of the ancient North American cratonic margin that are essential prerequisites to this style of post-collisional magmatism and associated gold-rich fluid exsolution.

Lamprophyre xenoliths

In addition to our research into the petrogenesis of post-collisional intrusive complexes at Scheelite Dome, Yukon, Canada, we also undertook a study of mafic-ultra mafic xenoliths we identified in calc-alkaline lamprophyre dikes in this region. As at Scheelite Dome, lamprophyres commonly occur as a late-stage intrusive phase in the Late Cretaceous igneous complexes that are otherwise dominated by felsic to intermediate potassic intrusions. The lamprophyres are dominantly minettes, but spessartites are also common.

At Clear Creek in the central Yukon, a series of xenoliths were sampled from a minette

dike. Two varieties were present. The first (Type 1), a medium to course-grained xenolith with an assemblage of clinopyroxene (augite) and phlogopite-biotite, in similar proportions. The second xenolith type is fine to medium grained, and predominantly Cr-rich diopside with minor phlogopite-biotite. A review of the literature indicates that similar xenoliths have been noted in association with similarly high K rocks in a variety of locations worldwide; however their origin remains enigmatic. The xenoliths could represent inclusions of mantle lithosphere sampled by the lamprophyres but unrelated to their genesis, mantle material that sourced the lamprophyres, or cognate xenoliths representing early crystallized material from the same parent melt that produced that lamprophyres. If the xenoliths represent accidental inclusions of metasomatized mantle, these xenoliths could provide insights into the geochemical evolution of the subcrustal mantle in this region and, ultimately, the source of Au incorporated into the Late Cretaceous granitic rocks.

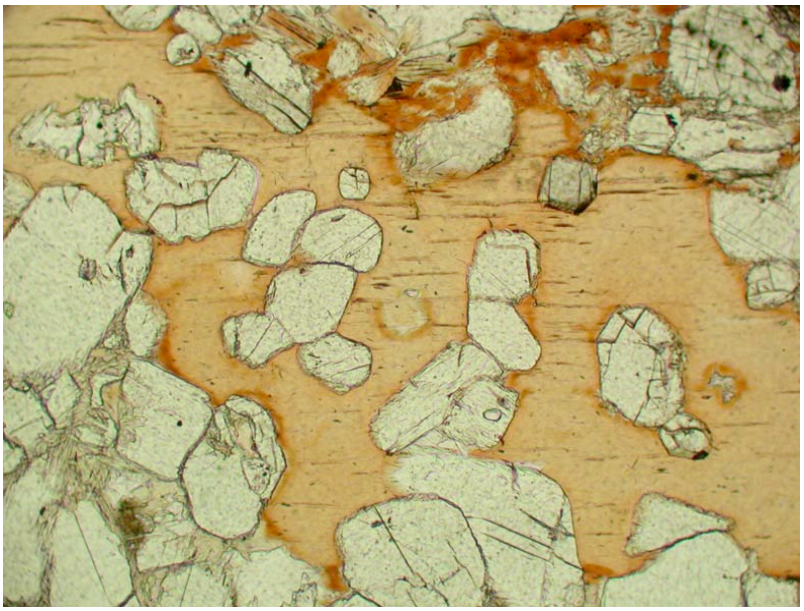

Fig. 5-Type 1 xenolith, consisting of ~ equal proportions of both phlogopite (brown) and clinopyroxene (augite). Field of view ~ 1cm in width.

The xenoliths generally have a cumulate texture, in some cases as pyroxene cumulates with phlogopite-biotite oikocrysts. Although the xenoliths are considerably more magnesian than the host lamprophyres, but have similar trace element characteristics with high LILE/HFSE ratios, and are enriched in light to middle REE. WDS analyses of biotite and pyroxene from the xenoliths indicate subtle but consistent variations in mineral chemistry. Minerals in Type 1 xenoliths feature less magnesian compositions,

but are relatively enriched in Al. Sr and Nd isotope data are similar for the xenoliths and host lamprophyres (and notably – also the more evolved intrusions; Fig. 6); however, the

Type	SAMPLE	Age (Ma)	Rb	Sr	$^{87}Rb/^{86}Sr$	$^{87}Sr/^{86}Sr_m$	$^{87}Sr/^{86}Sr_{(T)}$	Sm	Nd	$^{147}Sm/^{144}Nd$	$^{143}Nd/^{144}Nd_m$	$^{143}Nd/^{144}Nd_{(T)}$	$?_{Nd}(T)$	$T_{DM\ (Ga)}$
Clear Creek Lamprophyre 1	CC11 L-1	93	174	661	0.762	0.71243	0.71139	7.82	39.1	0.1210	0.512085	0.512009	-9.9	1.6
Cpx-phlogopite xenolith	CC11 X-1A	93	248	281	2.552	0.71467	0.71119	3.44	15.9	0.1310	0.512095	0.512013	-9.8	1.7
Cpx-phlogopite xenolith	CC11 X-3	93	202	288	2.030	0.71441	0.71164	3.65	17.1	0.1294	0.512104	0.512023	-9.6	1.7
Cpx-phlogopite xenolith	CC11 X-5	93	159	205	2.244	0.71441	0.71135	3.25	14.4	0.1366	0.512094	0.512008	-9.9	1.9
Clear Creek Lamprophyre 1	CC12 L-1	93	202	803	0.726	0.71256	0.71157	10.9	59.3	0.1114	0.512191	0.512121	-7.7	1.3
Cpx-phlogopite xenolith	CC12 X-2	93	271	387	2.025	0.71441	0.71164	8.19	42.6	0.1162	0.512137	0.512064	-8.8	1.4

Table 3- Nd and Sr isotope compositions and Rb, Sr, Sm and Nd concentrations (isotope dilution) for Clear Creek (Yukon) ultramafic xenoliths and their host lamprophyres

xenoliths feature slightly more radiogenic initial $^{87}Sr/^{86}Sr$ ratios than the host lamprophyres (Table 3).

A number of datasets have been generated from the xenolith samples, but their origin remains enigmatic. The isotope data suggests a possible genetic link between the host lamprophyres and the xenoliths. The strongly magnesian chemistry of the xenoliths, along with their cumulate and relatively high Sm/Nd ratios are all consistent with the possibility that these xenoliths represent cumulate minerals that precipitated from ultrapotassic melts similar to their host lamprophyres. However, data to unequivocally support this interpretation remain outstanding. Cr-diopside is unusual as a cumulate phase, and is more commonly described as a phase of low modal abundance in relatively refractory peridotite and so it remains possible that at least some of these xenoliths represent lithospheric mantle.

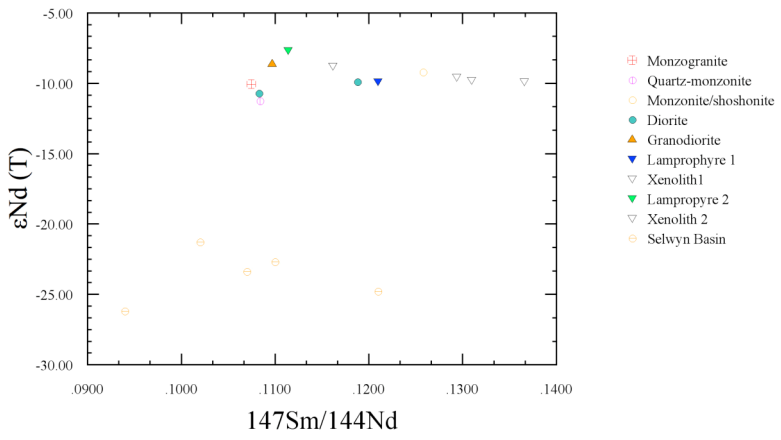

Fig. 6- Initial ε_{Nd} vs. $^{147}Sm/^{144}Nd$ for Clear Creek ultramafic xenoliths and host lamprophyres.

Microsamples Sr isotopic studies of feldspar phenocrysts, Fort Knox pluton, central Alaska

The ~93 Ma auriferous Fort Knox pluton is the prime gold producer in the Tintina Gold Belt in central Alaska and recent open pit mining has provided an unprecedented exposure of the intrusive igneous rocks likely related to the vein related gold-bismuth-tellurium sulfide mineralization found at this location.

Newly exposed in the base of the pit (in summer 2006) is porphyritic phase of the pluton characterized by alkali megacrysts (Fig. 8). These megacrysts are of interest because they main record variations in the magma body (or bodies) responsible for producing the Au rich hydrothermal fluids. As a result we undertook a detailed microchemical study of one such megacryst, with the intent to determine whether such megacrysts record changes in magma composition during the growth of the megacryst itself.

Although the grains contain no melt inclusions (as determined by Erin Marsh in Robert Bodnar's laboratory, VPI, in 2007), a PhD student at the University of Colorado (Mary Beth Cheversia) has demonstrated that significant measured Sr isotopic variations are preserved in this grain (Table 4; Fig. 9). The available data do not form a valid Sr isochron (Fig. 10), illustrating that the grain likely grew incrementally from distinct magma batches with different Sr isotopic composition, and that these isotopic differences were not completely erased during subsolidus reequilibration of grain.

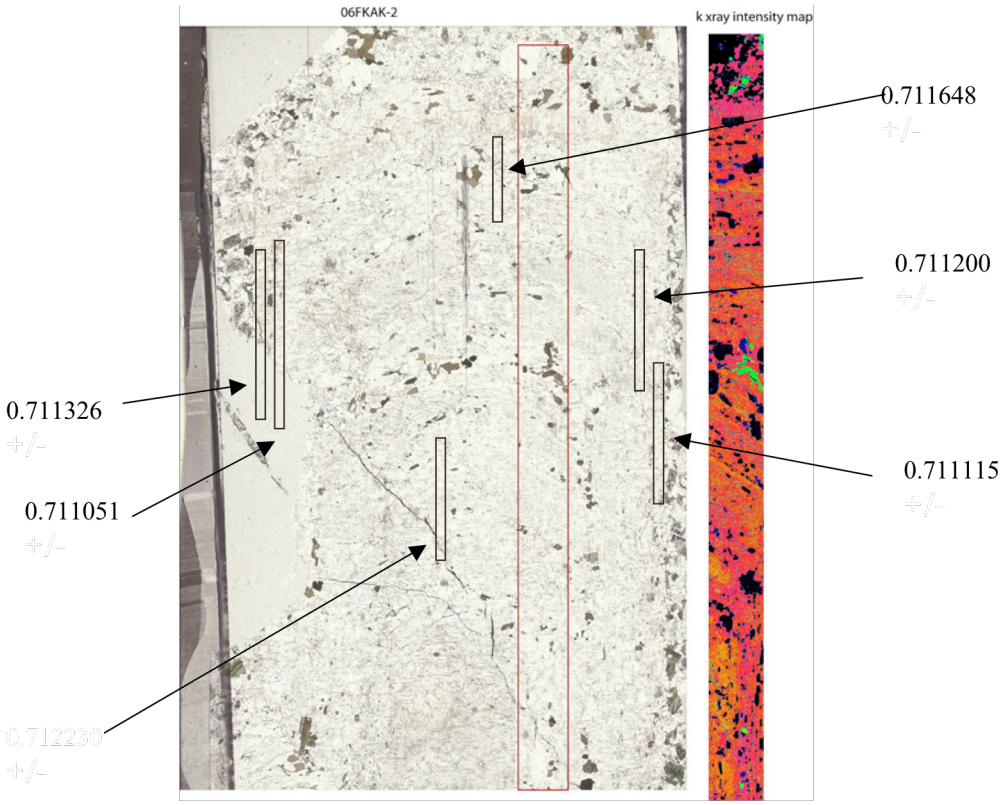

Fig. 9 Plane light (left) and electron microprobe (EMP) potassium X-ray intensity map (right) for Fort Knox feldspar megacryst. EMP analyses obtained at USGS (Denver) by Erin Marsh, and demonstrate considerable variability in feldspar potassium contents (red=high K, yellow=lower K contents). Boxes outlined in black on plane light photo are milling paths for physical microsamples (obtained using New Wave "Micromill" at University of Colorado, Boulder. Numbers shown are initial Sr isotopic composition for powders obtained from a given milling path. Red outlined box is position of that portion of the grain for which X-ray map was made.

Our initial data are not sufficiently resolved spatially to assess how the magma Sr isotopic compositions may have changed through time, but we are hoping to further resolve the Sr isotopic variations in this grain with smaller microsamples (permitted by high Sr contents of this grain, > 1000 ppm; Table 4). Once the isotopic compositions have been spatially resolved, we plan on additional EMP analyses of biotite inclusion to assess whether these trapped grains record their having grown in separate magma pulses. Eventually, trace element and volatile abundances in both the host feldspar and hydrous inclusions may allow us to reconstruct the magmatic and devolatilization history of the magmas parental to gold bearing veins at Fort Knox and so help better assess the conditions necessary to produce the gold depositing fluids. This work will represent part of the PhD studies by Mary Beth Cheversia at the University of Colorado and will be conducted over the next few years.

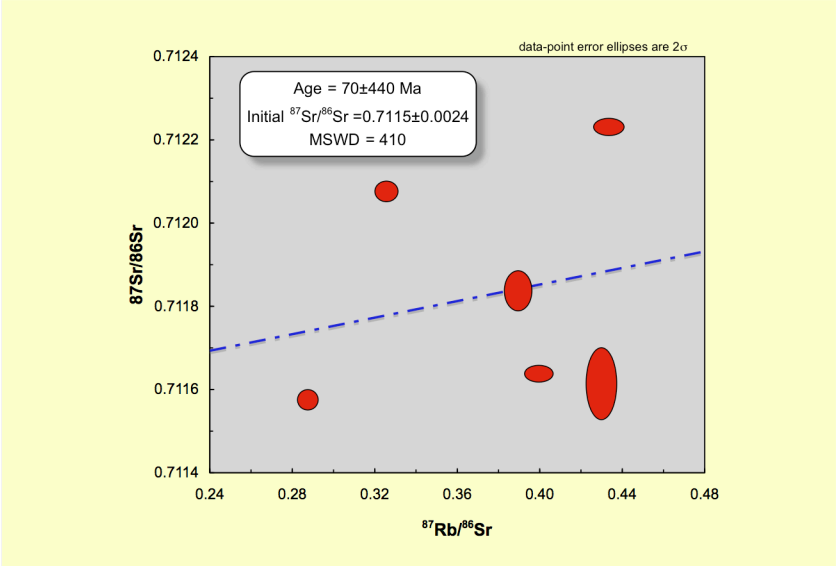

Figure 10- Microsample Sr isotopic data from feldspar megacryst from Fort Knox pluton. Error ellipses based on estimated errors from isotope dilution and isotopic analyses (Table 4). The scatter in $^{87}Sr/^{86}Sr$ observed in these samples is interpreted as evidence that feldspar grew from isotopically distinct magma batches.

Fort Knox feldspar megacryst	Rb (ppm)	Sr (ppm)	$^{87}Rb/^{86}Sr$	$^{87}Sr/^{86}Sr$ measured	$^{87}Sr/^{86}Sr$ unc 2σ	ng Sr analyzed
06FKAK2mbc-2	165	1225	0.390	0.711838	0.000039	196
06FKAK2mbc-3	265	1782	0.430	0.711616	0.00007	253
06FKAK2mbc-4	177	1178	0.434	0.71223	0.000017	117
06FKAK2mbc-5	144	1044	0.400	0.71164	0.000016	122
06FKAK2mbc-6	159	1596	0.287	0.711577	0.00002	54
06FKAK2mbc-7	175	1558	0.325	0.712076	0.00002	80

Table 4- Rb and Sr isotope dilution concentration determinations and Sr isotopic compositions of feldspar megacrysts from the Fort Knox pluton.